Fuzzy Logic Adjustment for Power Sharing in Wind and PV-based Isolated Microgrid

Lekhnath Kafle, Zhen Ni
Electrical Engineering and Computer Science Department
South Dakota State University
Brookings, SD, USA 57007
Email: {lekhnath.kafle, zhen.ni}@sdstate.edu

***Abstract*—Power flow control is one of the major issues in parallel connected inverters of an isolated microgrid. Droop control is considered to be the well-known method for managing power flows between micro-grid converters in decentralized manner. In this work, the fuzzy logic based improved droop control technique is developed to control the power flow between voltage source inverters connected in wind and solar photovoltaic (PV) based isolated low voltage AC microgrid. A proportional resonant (PR) voltage and current controllers are designed to control the current and voltage output of the voltage source inverter (VSI) connected with the dc battery. In the proposed micro-grid model, one battery is associated with wind turbine generator (WTG) system and another battery with PV system. The fuzzy logic controller (FLC) adjusts the droop coefficient values of the VSI connected with each DC battery according to its state of charge (SOC) and the power difference between total load and renewable generation. This technique demonstrates the robustness of the control system even in sudden load change condition and improves the system frequency response in wind and PV based isolated microgrid.**

***Index Terms*—Power sharing, Photovoltaic and wind power sources, Computational intelligent, Fuzzy logic, Isolated mode, Microgrid**

I. Introduction

Today, an estimated 17 % of the world population, or 1.2 billion people, live without access to electricity, and 80% of these people live in rural area [1]. Isolated microgrid with renewable energy sources and battery storage system is an adequate solution to supply power in such remote places where access to a large interconnected grid is limited [2]. Among various renewables, wind turbine generation (WTG) and Photovoltaic (PV) systems are expected to play important roles as clean sources in meeting future demand. The combination of wind and PV is more economical to run and provide better reliability [3]. The weakness of one system can be compensated by the strength of the other. Such combination improves the overall economy and reliability of renewable power generation. In isolated hybrid system, the renewable sources and energy storage systems are connected in a common AC bus through power electronics converters. For inverter based isolated microgrid, the control objective is to achieve accurate power sharing while maintaining system frequency and voltage within acceptable range of operation. The droop control is widely accepted technique used to obtain accurate load sharing among parallel inverters, without communication system. Droop control loops (P - ω and Q - E droops) have been applied to connect inverters in parallel in uninterruptible power supply (UPS) system to obtain good power sharing [4], [5]. Since this technique does not need any control wire connection, it is often known as wireless or independent parallel control [6]. With this technique, however, power sharing is obtained through voltage and frequency deviation of the system. That means the output frequency and voltage magnitude drop when the active and reactive power delivered by the inverter increases [7]. Thus, the purpose of droops is to keep power balance and to control the voltage and the frequency in the isolated microgrid.

A droop control is generally applied for multi-converter based isolated microgrid system using proportional integral (PI) controllers in voltage and inner current control loops. PI controller has several drawbacks. It is not able to track a sinusoidal reference without steady state error so voltage feed-forward term is needed to obtain good dynamic response [8]. Synchronous frame PI controller with voltage feed forward needs d-q transformation which increases the computation burden. Also, the imperfect compensation action of the feed forward control ultimately results in high harmonic distortion of the current. These problems are mitigated by using stationary frame proportional resonant (PR) controller that easily tracks reference signals and eliminates steady state errors in resonant frequency [9]. The complete design guidelines for PR controller based inner current/voltage loop is presented in [10].

A comprehensive overview on various computational intelligence (CI) applications in different contexts of power grid is presented in [11]. Fuzzy logic system is one of the CI technique that can combine regulation algorithms and logical reasoning to facilitate the control of complicated and uncertain system [12]. The fuzzy logic controller (FLC) is developed to improve the dynamic performance of the isolated wind and diesel hybrid microgrid in [13]. In this work, FLC is used to control the thyristor switches of additional sets of three phase resistive load connected in the network for the purpose of frequency control. The fuzzy logic based pitch angle controller is developed in [14] for reducing the output power fluctuation of WTG system in order to reduce the frequency fluctuation of isolated microgrid. The optimal load sharing control between multiple inverters connected in smart

house is achieved in [15] using droop control and fuzzy control methods. The optimal load sharing is achieved by changing the droop characteristics of each inverter connected to PV system, storage battery, and electric vehicle (EV) in smart home. The proper load current sharing is achieved using FLC in [16] for parallel DC-DC converter operation in low-voltage DC microgrid. In this method, the FLC calculates the virtual resistance instantly, based on output voltage deviation of converters, providing proper load current sharing, improving load voltage and decreasing circulating current between the converters.

In this paper, FLC adjusts the droop coefficient values of the VSI connected to each DC battery of PV and WTG systems of an isolated microgrid. As a result, VSI connected to each battery system share the load according to the SOC of the battery, renewable generation and load profile. In this case, the FLC calculates the adjustment factor that is used to update droop coefficient value. The batteries connected to each renewable generation share the load according to their updated droop coefficients. This method is tested in a low voltage AC connected wind and PV based isolated microgrid. The simulation results validate the advantages and importance of FLC for the better performance of wind and PV based isolated microgrid.

The rest of the paper is organized as follows: Section II describes the microgrid system model with renewable energy sources. The microgrid control system structure along with FLC is explained in section III. The simulation result is presented and discussed in section IV. Finally, the conclusion is drawn based on result.

II. System Model with Renewable Energy Sources

The system block diagram of an AC isolated microgrid model is depicted in Figure 1, which consists of WTG and solar PV generation system along with inverter interfaced batteries. Each renewable source is connected to the common AC bus through power electronics converters. As the WTG and solar PV sources operate under maximum power point tracking (MPPT), they can be emulated as three-phase current sources feeding directly to the loads, and the inverter interfaced battery acts as a voltage source that controls the AC bus voltage. Each battery is associated with each renewable generation. One battery is connected to PV generation and another is connected to WTG system. Each configuration (PV+ESS or WTG+ESS) is connected to a common AC bus. The different droop coefficients are assigned to different batteries in order to share the load differently. The VSI control mechanism regulates the magnitude and frequency of the system voltage.

In this system model, batteries play important role to guarantee a continuous supply of power. A battery is charged when total renewable generation is higher than total load demand. Whereas, it is discharged when total renewable generation is lower than total load demand.

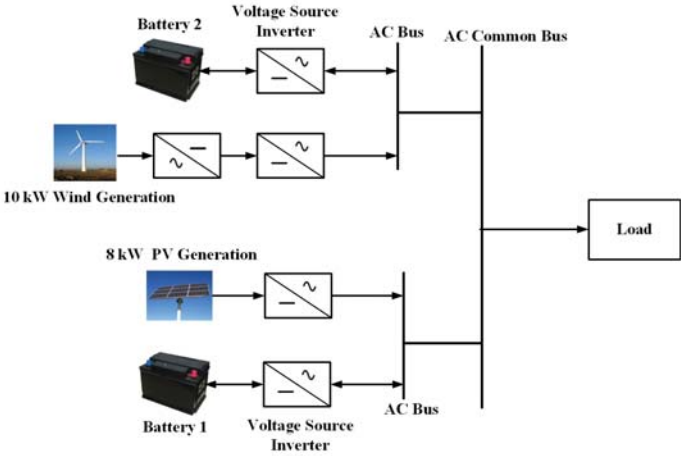

Fig. 1. Hybrid wind and solar PV based stand-alone microgrid model with battery

A. Renewable Energy Sources Modeling

The output power from renewable energy sources depends on the weather conditions. The power from WTG mainly depends on wind speed, whereas power from solar PV depends on the intensity of incident radiation. These renewable energy sources can be emulated as controlled current sources. In our system model, WTG and solar PV systems are modeled using three controlled current sources that have no inertial response and thus providing easier implementation and faster simulation processes.

The inputs to the wind module are the wind speed values followed by wind turbine power curve and instantaneous values of the reference three-phase voltage.

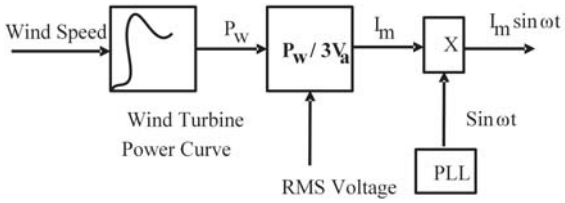

Fig. 2. Per Phase Wind System Model

Similarly, the inputs to the PV module are the percentage of normalized irradiance value, the peak PV size, and the instantaneous value of the reference three phase voltage.

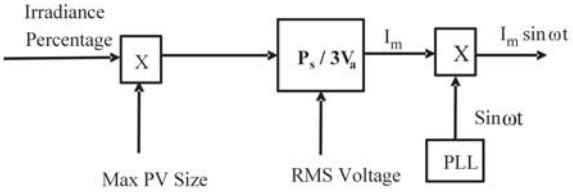

Fig. 3. Per Phase PV System Model

In both modules, the efficiency of the system is assumed to be 100% and reference voltage is the common AC bus voltage of the microgrid system to which WTG and solar PV have to

be connected. This voltage provides the phase information for the WTG and PV solar system, so that the output voltage (or current) of both modules are in the same phase as the reference voltage. The phase information can be obtained with the help of phase locked loop (PLL).

III. Control System Design

The battery is connected to a common AC bus through a bidirectional converter known as voltage source inverter (VSI). VSI can generate the sinusoidal voltage waveform of desired frequency and voltage magnitude. The block diagram of VSI controller with droop control loop is shown in Figure 4.

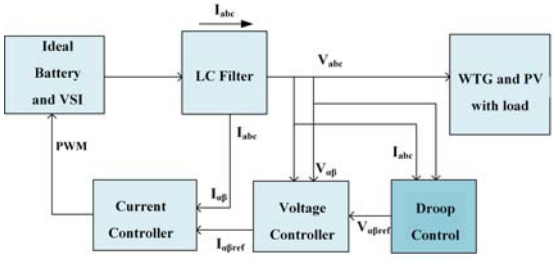

Fig. 4. Control block diagram for VSI with droop control

The VSI controller consists of three control loops: current control loop, voltage control loop and droop control loop. Current control loop is the loop around the filter inductor and VSI, which acts as control current source and regulates the output current from the VSI. Voltage control loop is around the filter capacitor and VSI, which behaves like a controlled voltage source and controls the output voltage from VSI. The droop control loop generates voltage magnitude and frequency reference set points for generation of the reference three-phase voltage. The three-phase system is modeled as two independent single phase systems using Clarke's transformation principle (abc to $\alpha\beta$). The LC filter is connected to the output of VSI to eliminate the current ripples caused by switching of the inverter.

1) Droop Loop Design: According to the droop principle, control of frequency dynamically controls the power angle, and, thus, the real power flow. The principle also states that control of difference in voltage magnitude controls the reactive power flow from the inverter. When the load increases in a micro-grid, active power and reactive power output from the inverter has to be increased. As a result, the system frequency and voltage level drops due to droop characteristics. The droop lines for active and reactive power control is illustrated in Fig. 5 and described by equations (6 and 2). The acceptable range for frequency and voltage drop can be defined to maintain the frequency and voltage of such remote micro-grid within pre-defined limits.

$$\omega_{ref} = \omega_{nL} + mP \tag{1}$$

$$V_{ref} = V_{nL} - nQ \tag{2}$$

where ω_{ref} and V_{ref} are angular frequency and voltage magnitude references respectively, ω_{nL} and V_{nL} are no load angular frequency and no load voltage, respectively. P_0 and Q_0 are output active and reactive power respectively, and m and n are the active and reactive droop coefficients respectively.

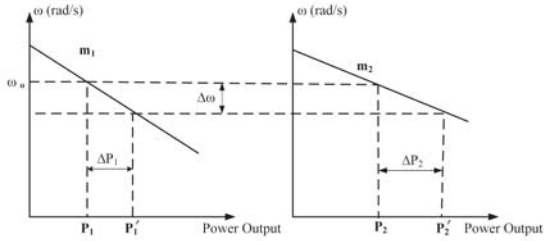

Fig. 5. Droop lines for active and reactive power

When two inverters are connected in parallel, they share the portion of the active power according to their droop coefficient values. The active droop lines for two parallel inverter is shown in 5. Let's assume that the slope of droop line of active power for the first inverter (m_1) is higher than that of the slope of the second inverter (m_2). The active power shared by these inverters can be expressed as:

$$\Delta P_1 = P_1^{'} - P_1 = \frac{\Delta f}{m_1} \tag{3}$$

and

$$\Delta P_2 = P_2^{'} - P_2 = \frac{\Delta f}{m_2} \tag{4}$$

Therefore,

$$\frac{\Delta P_1}{\Delta P_2} = \frac{m_2}{m_1} \tag{5}$$

Equation 5 shows the droop coefficient ratio of the two inverters is inversely proportional to their power sharing ratio. Thus, the inverter with lower droop value would take large amount of load and inverter with higher droop value would take less amount of load.

The basic operation of the droop control block is to provide voltage magnitude and frequency reference. First, output voltage and current of the inverter are used to compute instantaneous active power (P) and instantaneous reactive power (Q) in α β reference frame. Next, average active and reactive power corresponding to the fundamental component are obtained by means of low pass filter. Finally, the droop equations (6 and 2) are used to compute reference parameters to generate three phase reference voltage. All the steps are shown in Figure 7.

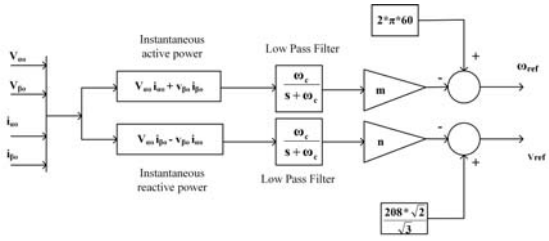

Fig. 6. Droop controller block diagram

The three-phase reference voltage signal is generated from voltage magnitude and frequency reference obtained from the droop controller loop. It is then compared with the measured three-phase voltage signal. The compared value fed into the controller to obtain the sinusoidal control signal for the PWM of the inverter.

2) Fuzzy Logic Controller: Fuzzy logic is a precise problem solving methodology that is based on how human thinks. The FLC converts a linguistic control strategy based on expert knowledge into an automatic control strategy [17]. FLC is able to simultaneously handle the numerical data and linguistic knowledge. It facilitates the control of complicated system without knowledge of its mathematical description [18]. Fuzzy logic consists of four main parts: fuzzification, rules, inference engine and defuzzification. First step is fuzzification in which a crisp set of input data are collected and converted into a fuzzy set using fuzzy linguistic terms and membership functions. Second step is to make an inference using set of rules. The rule is constructed to control the output variable of FLC. A fuzzy rule is simply IF-THEN rules with the condition and conclusion. Last step is defuzzification in which the resulting fuzzy output is mapped to a crisp output using the membership functions [19]. Defuzification can be performed according to the membership functions of output variables. There are various method of defuzzification such as center of gravity, center of gravity for singletons, left most maximum and right most maximum. Among them center of gravity method is highly popular.

In this case, FLC adjusts the droop coefficient values of the VSI controller based on SOC of the battery and the power difference between total renewable generation and load demand.

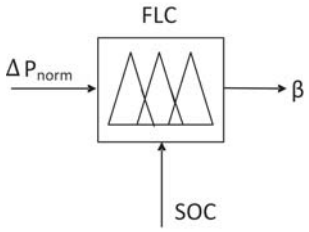

Fig. 7. Fuzzy Logic controller

The FLC has five input triangular membership functions for SOC of the battery: very small (VS), small (S), medium (M), big (B), very big (VB). Also, for input normalized power deviation has seven triangular membership functions: negative big (NB), negative small (NS), zero (ZR), positive small (PS), positive medium (PM), positive big (PB). The output also has seven membership functions: NB, NM, NS, ZR, PS, PM, PB.

The FLC provides the seven different thirty five output values which adjusts the droop coefficients values of two different inverters so that they can share the load according to their SOC and the power deviation in micro-grid. The FLC output is represented by β whose values range between -1 and 1. This adjustment factor can be incorporated in the droop

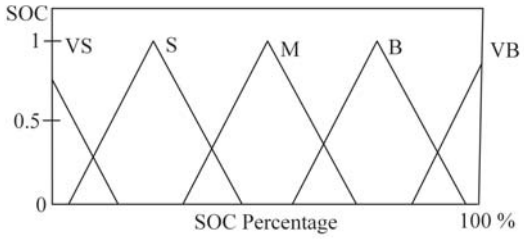

Fig. 8. Membership function for SOC

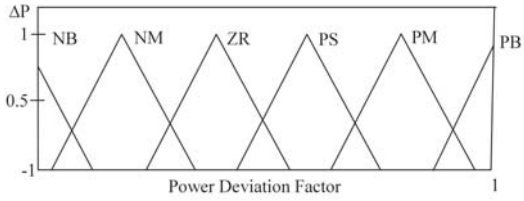

Fig. 9. Membership function for power deviation

equation so that active droop equation can be modified as follows:

$$\omega_{ref} = \omega_{nL} + (\frac{m}{\beta})P \tag{6}$$

Thus, the amount of power shared by battery in each renewable source depends on the value of β . The battery is charged when β is positive and discharged when β is negative.

IV. Simulation Result

The isolated microgrid system model presented in figure 1 was used for the test system. The microgrid model consists of 10 kW of WTG system and 8 kW of PV generation system. Both renewable energy sources were emulated through three-phase controlled current sources. The maximum power from the first inverter and second inverter are assumed to be 7000 Watt and 15000 Watt respectively. The maximum allowable frequency change is assumed to be $\pm 2\%$ of nominal frequency. Based on those information, the droop coefficients for both VSIs can be calculated. The simulation was run for 1 s in MATLAB/SIMULINK. Load is increased from 19 kW to 22 kW at t= 0.5 sec. Throughout the simulation time, the output power from the renewable energy sources is assumed to be constant. The output power from the renewable sources and the step change in load power is depicted in figure 11. The red line shows the step change in load. The black and blue lines show the output power from WTG and PV generation systems respectively.

A. Case I: Battery 1 with 100% SOC and Battery 2 with 60% SOC

In this case, the two batteries with PV and WTG systems are set to have SOC of 100% and 60% respectively. Since, the available total renewable generation is 18 kW, 1 kW load is shared by two batteries up to t= 0.5 sec. As the load is increased to 22 kW after t=0.5 sec, two batteries share 4 kW

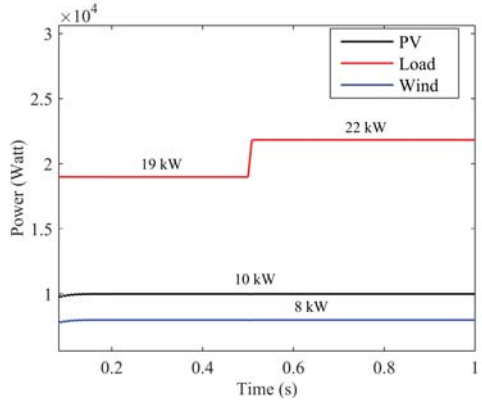

Fig. 10. Step change of load and renewable generation

of deficient power. The active power shared by both batteries is shown in Figure 11. The black and red lines represents the active power shared by the battery one with 100% SOC and battery two with 60% SOC during load change condition. In this condition, the droop adjustment factors are found to be 0.66 and 0.39 for batteries in the PV and WTG systems respectively.

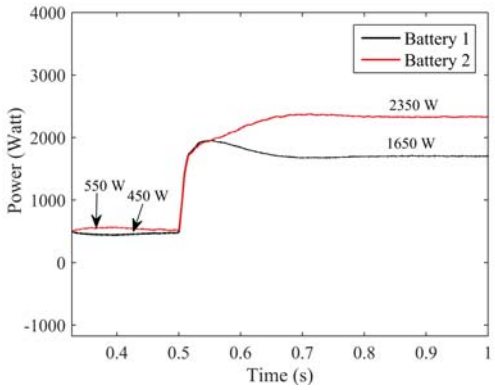

Fig. 11. Output power from batteries when battery 1 with 100% SOC and battery 2 with 60% SOC

The first and second batteries provide 450 W and 550 W active power during 1 kW of deficit power and 1650 W and 2350 W of deficit power during 4 kW of deficit power in the microgrid system. The sharing ratio is approximately same in both cases.

B. Case II: Battery 1 with 60% SOC and Battery 2 with 100% SOC

In this case, the SOC of first battery is reduced and SOC of second battery is increased. The SOC of first and second batteries are set to 60% and 100% respectively. The active power shared by both batteries is depicted in Figure 12. In this condition, the output from the FLC (β) is found to be 0. The active power shared by batteries one and two is represented by black and red lines respectively. In this case also, the sharing ratio is found to be approximately equal before and after load change. The amount of power shared by both batteries is also provided in 12.

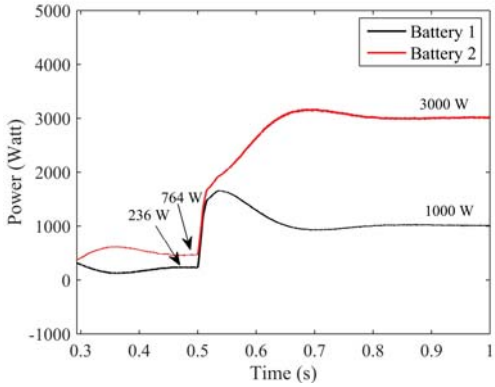

Fig. 12. Output power from batteries when battery 1 with 100% SOC and battery 2 with 60% SOC

After conducting the simulations for two different cases, the output power from each battery is compared with different SOC at different load conditions. Batteries are able to share the load according to their SOC and deficit amount of power in the system. Output power from each battery with 100% SOC and 60% SOC is shown in figure 13 and 15. In this condition, the values of droop adjustment factors are found to be 0.39 and 0.66 for batteries in the PV and WTG systems respectively. Since the deficient power is 1 kW before and 4 kW after t= 0.5 sec, the batteries have to supply required amount of power to balance generation and consumption.

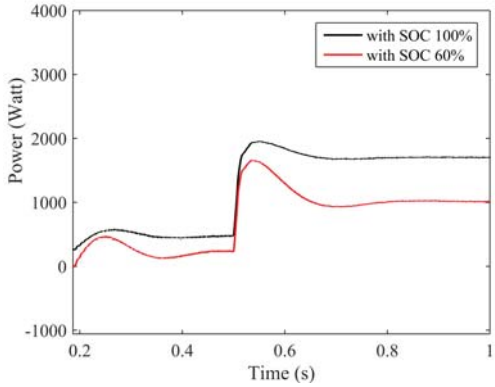

Fig. 13. Output power from battery with PV system

It can be clearly seen that battery with 100% SOC provides more power than battery with 60% SOC. The designed control system is able to share the load according to the amount of deficit power in the system and available energy in the battery.

With the help of fuzzy logic controller the power sharing between parallel inverters connected to storage systems is improved. It is observed that the drooping of frequency is higher if SOC of the batteries and deficient and sufficient power in the system is not considered. The black line shows the frequency response without fuzzy logic controller and the

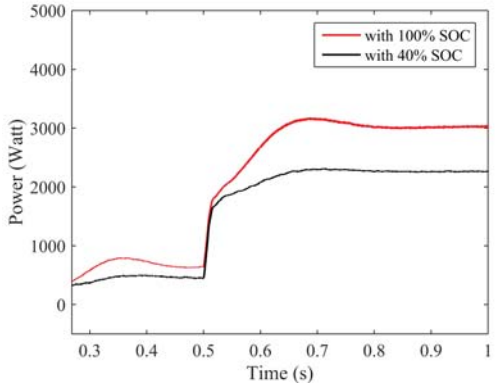

Fig. 14. Output power from battery with WTG system

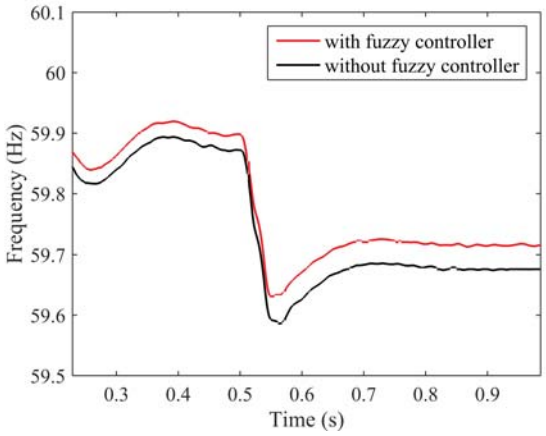

Fig. 15. Comparison of frequency response with and without fuzzy controller

red line shows the improved frequency response with the help of droop controller.

V. Conclusion

In this paper, the droop coefficients are adjusted in the storage systems of wind and PV-based isolated microgrid using FLC. The improved power sharing between storage systems are achieved considering the SOC of the battery and power difference between total load and renewable generation. The FLC is able to adjust the droop coefficient according to the energy available in the battery and deficient and surplus power in the system. Batteries can supply high amount of power with high SOC and low amount of power with low SOC. This means the SOC level affects the active power contribution from each battery in order to balance supply and demand. The FLC adjusted the droop coefficient of PR controller of storage system thereby improving the frequency response of the system by 0.067%. In order to improve the accuracy of the result, multiple test cases could be conducted for frequency comparison. This technique showed robustness even in the case of sudden load change conditions.

Acknowledgement

This work was supported by the National Aeronautics and Space Administration (NASA) under award No. NNX15AK54A.

References

[1] F. Birol, "World energy outlook 2010," *International Energy Agency*, vol. 1, 2010.

[2] R. H. Lasseter, J. H. Eto, B. Schenkman, J. Stevens, H. Vollkommer, D. Klapp, E. Linton, H. Hurtado, and J. Roy, "Certs microgrid laboratory test bed," *IEEE Transactions on Power Delivery*, vol. 26, no. 1, pp. 325–332, 2011.

[3] R. A. Badwawi, M. Abusara, and T. Mallick, "A review of hybrid solar pv and wind energy system," *Smart Science*, vol. 3, no. 3, pp. 127–138, 2015.

[4] J. M. Guerrero, N. Berbel, L. G. de Vicuña, J. Matas, J. Miret, and M. Castilla, "Droop control method for the parallel operation of online uninterruptible power systems using resistive output impedance," in *Twenty-First Annual IEEE Applied Power Electronics Conference and Exposition, 2006. APEC'06.*, pp. 7–pp, IEEE, 2006.

[5] J. M. Guerrero, J. C. Vasquez, J. Matas, L. G. De Vicuña, and M. Castilla, "Hierarchical control of droop-controlled ac and dc microgridsa general approach toward standardization," *IEEE Transactions on Industrial Electronics*, vol. 58, no. 1, pp. 158–172, 2011.

[6] C.-C. Hua, K.-A. Liao, and J.-R. Lin, "Parallel operation of inverters for distributed photovoltaic power supply system," in *Power Electronics Specialists Conference, 2002. pesc 02. 2002 IEEE 33rd Annual*, vol. 4, pp. 1979–1983, IEEE, 2002.

[7] P. Villenueve, "Concerns generated by islanding [electric power generation]," *Power and Energy Magazine, IEEE*, vol. 2, no. 3, pp. 49–53, 2004.

[8] R. Teodorescu, F. Blaabjerg, U. Borup, and M. Liserre, "A new control structure for grid-connected lcl pv inverters with zero steady-state error and selective harmonic compensation," in *Applied Power Electronics Conference and Exposition, 2004. APEC'04. Nineteenth Annual IEEE*, vol. 1, pp. 580–586, IEEE, 2004.

[9] R. Teodorescu, F. Blaabjerg, M. Liserre, and P. C. Loh, "Proportional-resonant controllers and filters for grid-connected voltage-source converters," in *Electric Power Applications, IEE Proceedings*, vol. 153, pp. 750–762, IET, 2006.

[10] H. Gu, D. Wang, H. Shen, W. Zhao, and X. Guo, "New power sharing control for inverter-dominated microgrid based on impedance match concept," *The Scientific World Journal*, vol. 2013, 2013.

[11] R. G. Harley and J. Liang, "Computational intelligence in smart grids," in *IEEE Symposium Series on Computational Intelligence (SSCI)*, pp. 11–15, 2011.

[12] R. B. Menon, S. B. Menon, D. Srinivasan, and L. Jain, "Fuzzy logic decision-making in multi-agent systems for smart grids," in *Computational Intelligence Applications In Smart Grid (CIASG), 2013 IEEE Symposium on*, pp. 44–50, IEEE, 2013.

[13] M. Marzband, A. Sumper, O. Gomis-Bellmunt, P. Pezzini, and M. Chindris, "Frequency control of isolated wind and diesel hybrid microgrid power system by using fuzzy logic controllers and pid controllers," in *Electrical Power Quality and Utilisation (EPQU), 2011 11th International Conference on*, pp. 1–6, IEEE, 2011.

[14] R. M. Kamel, A. Chaouachi, and K. Nagasaka, "Three control strategies to improve the microgrid transient dynamic response during isolated mode: A comparative study," *IEEE Transactions on Industrial Electronics*, vol. 60, no. 4, pp. 1314–1322, 2013.

[15] M. Miyagi, S. Morinaga, Y. Shiroma, and T. Funabashi, "Optimal load sharing using droop control and fuzzy control in uninterruptible smart house," in *Future Energy Electronics Conference (IFEEC), 2013 1st International*, pp. 103–108, IEEE, 2013.

[16] N. L. Diaz, T. Dragičević, J. C. Vasquez, and J. M. Guerrero, "Fuzzy-logic-based gain-scheduling control for state-of-charge balance of distributed energy storage systems for dc microgrids," in *2014 IEEE Applied Power Electronics Conference and Exposition-APEC 2014*, pp. 2171–2176, IEEE, 2014.

[17] C.-C. Lee, "Fuzzy logic in control systems: fuzzy logic controller. ii," *IEEE Transactions on systems, man, and cybernetics*, vol. 20, no. 2, pp. 419–435, 1990.

[18] E. H. Mamdani and S. Assilian, “An experiment in linguistic synthesis with a fuzzy logic controller,” *International journal of man-machine studies*, vol. 7, no. 1, pp. 1–13, 1975.
[19] J. M. Mendel, “Fuzzy logic systems for engineering: a tutorial,” *Proceedings of the IEEE*, vol. 83, no. 3, pp. 345–377, 1995.